Accurate and Efficient Solutions of Compressible Internal Flows

A. Dadone* and M. Napolitano†
Universitá degli studi di Bari, Bari, Italy

This paper applies a new perturbative lambda formulation to one- and two-dimensional compressible internal flows. The lambda Euler equations are recast in terms of perturbation-type variables, which are the differences between the usual characteristic (Riemann) variables and those corresponding to an appropriate incompressible flow. In this way, the geometry-induced gradients are accounted for by the incompressible flow solution and the rather smooth correction due to the compressibility effects, can be solved accurately with even a very coarse mesh. The perturbative equations are provided for the cases of one- and two-dimensional flows and are solved numerically by means of a fully implicit and an alternating direction implicit method, respectively. The accuracy and efficiency of the proposed approach are demonstrated by means of a few example/applications.

Introduction

STEADY as well as unsteady compressible flow phenomena play a very significant role in most propulsive applications of engineering interest and have been the subject of many theoretical and experimental studies. Due to the spectacular developments in computer hardware and software in the last few decades, numerical simulation has become a very useful and widespread tool for predicting compressible flows in complex geometries of practical relevance.

Among the several numerical methods developed for computing compressible inviscid flows, the so-called lambda formulation, recently developed and employed by Moretti et al.,[1,2] has several very desirable features. The time-dependent compressible Euler equations are recast in terms of compatibility conditions for characteristic (Riemann) variables along characteristic lines and discretized by means of upwind differences that correctly take into account the direction of wave propagation. In this way, a numerical technique is obtained, which combines the coding simplicity of finite difference methods with the intrinsic accuracy and physical soundness of the method of characteristics. Since its first appearance as a working tool for solving compressible flows numerically,[1] the lambda formulation has undergone several improvements. The authors have developed various implicit integration schemes[3-5] in order to enhance the efficiency of the lambda methodology by removing the CFL stability limitation of the explicit schemes employed previously.[1,2] Also, when solving two-dimensional compressible flows in a general orthogonal curvilinear coordinate system,[4] they have shown that a significant improvement in the accuracy of the solution is obtained by employing the incompressible potential flow net as the computational grid for the numerical calculation of the compressible flow. In this way, a desired accuracy level can be achieved using a coarser grid, that is, at a lower computation cost. A noteworthy contribution toward improving the efficiency of the lambda methodology for computing steady flows has recently been provided by Moretti, who devised appropriate implicit relaxation methods for both one- and two-dimensional flows.[6,7] In particular, for the case of one-dimensional steady flows, Moretti has shown that a box-type spatial discretization is the one that best mimics the method of characteristics and provides considerably more accurate results than those obtained by means of any other second-order-accurate spatial discretization. Moreover, he has developed a simple and effective shock-tracking procedure that correctly locates and moves shocks of arbitrary strength.[6]

This paper provides a further improvement of the lambda methodology by combining all of the aforementioned advances with a new perturbative approach. The idea of employing perturbation-type equations[8]—which has been independently implemented by other authors in a more general context[9]—is indeed the most natural and logical development of the method proposed in Ref. 4. In fact, if the incompressible potential flow net is used as a very suitable computational grid,[4] so that an accurate incompressible flow solution is available at no extra cost, it is convenient to reformulate the governing equations in terms of new variables, which are the differences between those corresponding to the sought compressible flow and those corresponding to the known incompressible one. In this way, the geometry-induced gradients are mostly accounted for by the incompressible flow solution and the perturbative problem, which is smoother and better behaved than the full compressible one, can be solved very accurately even on a coarse grid.

The advantage of such an approach is paramount when computing flows having one or more stagnation points, around which very large geometry-induced gradients are present; see, for example, Ref. 10, which provides some airfoil flow calculations by means of the present perturbative lambda formulation. Here, the proposed approach is tested vs one- and two-dimensional internal flows, which are more relevant to propulsion applications. For the case of one-dimensional flows, the new formulation, combined with the implicit integration scheme of Ref. 3 and employing the box-type spatial discretization as well as the shock-tracking procedure due to Moretti,[6] will be shown to provide an extremely accurate and efficient technique. For the case of two-dimensional flows, the present approach, using a simplified version of the alternating direction implicit (ADI) scheme proposed by the authors,[3,4] will be seen to produce more accurate results than those obtained by means of the already very accurate method of Ref. 4, even in the absence of large geometry-induced gradients.

One-Dimensional Flows

Numerical Method

For the case of quasi-one-dimensional isentropic flows, the lambda formulation equations are given in dimensionless

Presented as Paper 84-1247 at the AIAA/SAE/ASME 20th Joint Propulsion Conference, Cincinnati, OH, June 11-13, 1984; received Aug. 26, 1984; revision received July 26, 1985.

*Professor, Istituto di Macchine.
†Professor, Istituto di Macchine. Member AIAA.

form as[1,2]

$$C_t + \lambda_c C_x = -\alpha u a \tag{1}$$

$$D_t + \lambda_d D_x = \alpha u a \tag{2}$$

where u and a are the speeds of the fluid and of the sound, respectively, α is the specific rate of change of the cross-sectional area $W(\alpha = W_x/W)$, and the subscripts x and t indicate partial derivatives with respect to the longitudinal coordinate x and time t. C and D are the two characteristic (Riemann) variables and λ_c and λ_d are the slopes of the corresponding characteristic lines, namely

$$C = u + \zeta a \tag{3}$$

$$D = u - \zeta a \tag{4}$$

$$\lambda_c = u + a \tag{5}$$

$$\lambda_d = u - a \tag{6}$$

with $\zeta = 2/(\gamma - 1)$, γ being the specific heats ratio of the perfect gas under consideration.

Let us now consider a new set of perturbative dependent variables, namely

$$\bar{u} = u - u', \qquad \bar{a} = a - a' \tag{7a,b}$$

$$\bar{C} = C - C', \qquad \bar{D} = D - D' \tag{7c,d}$$

In Eqs. (7), u' and a' are the solution of the following steady "incompressible flow" equations

$$u' W = \text{const} \tag{8}$$

$$u'^2 + \zeta a'^2 = \zeta a_0^2 \tag{9}$$

where a_0 is the total (stagnation) speed of sound of the considered compressible steady flow, and C' and D' are obtained from u' and a' by means of equations formally identical to Eqs. (3) and (4).

Equations (1) and (2) are then written in terms of the new perturbative variables, to give

$$\bar{C}_t + \lambda_c \bar{C}_x = -k1\bar{a} - k2\bar{u} - \alpha\bar{u}\bar{a} - k4 \tag{10}$$

$$\bar{D}_t + \lambda_d \bar{D}_x = -k1\bar{a} - k3\bar{u} + \alpha\bar{u}\bar{a} + k4 \tag{11}$$

where $k1$, $k2$, $k3$, and $k4$ are given as

$$k1 = \zeta a'_x \tag{12}$$

$$k2 = u'_x + \alpha a' + k1 \tag{13}$$

$$k3 = u'_x - \alpha a' - k1 \tag{14}$$

$$k4 = k1 u' \tag{15}$$

It is noteworthy that $k1$, $k2$, $k3$, and $k4$ are known coefficients that depend only on the incompressile flow solution and are therefore constant with respect to time. Also, in Eqs. (10) and (11), the unknown dependent variables are all perturbations with respect to the incompressible flow solution, except for λ_c and λ_d, which are the slopes of the physical characteristic lines, that is, those corresponding to the complete compressible flow solution, u and a. Therefore, Eqs. (10) and (11) can be interpreted as compatibility conditions for "perturbative disturbances."

Equations (10) and (11) are discretized in time by means of a two-level implicit backward Euler scheme, using the delta (Δ) approach of Beam and Warming,[11] and linearized in time by neglecting terms of order Δ^2, to give

$$\Delta C/\Delta t + \lambda_c^n \Delta C_x + \bar{C}_x^n(\Delta u + \Delta a) + k1\Delta a + k2\Delta u + \alpha(\bar{u}^n \Delta a + \bar{a}^n \Delta u) = -\lambda_c^n \bar{C}_x^n - k1\bar{a}^n - k2\bar{u}^n - \alpha\bar{u}^n\bar{a}^n - k4 \tag{16}$$

$$\Delta D/\Delta t + \lambda_d^n \Delta D_x + \bar{D}_x^n(\Delta u - \Delta a) + k1\Delta a + k3\Delta u - \alpha(\bar{u}^n \Delta a + \bar{a}^n \Delta u) = -\lambda_d^n \bar{D}_x^n - k1\bar{a}^n - k3\bar{u}^n + \alpha\bar{u}^n\bar{a}^n + k4 \tag{17}$$

In Eqs. (16) and (17), the superscript n indicates variables that are evaluated at the old time level t^n explicitly, whereas Δ indicates time increments of the perturbative variables from the old time level t^n to the new time level, $t^{n+1} = t^n + \Delta t$, namely,

$$\Delta C = \bar{C}^{n+1} - \bar{C}^n, \qquad \Delta D = \bar{D}^{n+1} - \bar{D}^n \tag{18a,b}$$

$$\Delta u = \bar{u}^{n+1} - \bar{u}^n, \qquad \Delta a = \bar{a}^{n+1} - \bar{a}^n \tag{18c,d}$$

Equations (16) and (17) are rewritten in such a way as to eliminate the Δu and Δa variables in terms of ΔC and ΔD by means of the following relationships:

$$\Delta u = (\Delta C + \Delta D)/2 \tag{19}$$

$$\Delta a = (\Delta C - \Delta D)/2\zeta \tag{20}$$

which can be obtained very easily from Eqs. (3), (4), (7), and (18). The resulting equations—which are omitted here for the sake of conciseness—are discretized in space by means of a two-point second-order-accurate upwind box scheme: all of the terms in Eq. (16) are evaluated at the center of the mesh immediately preceding the x_i gridpoint, that is,

$$\Delta C/\Delta t = (\Delta C_i + \Delta C_{i-1})/2\Delta t \tag{21}$$

$$\lambda_c = (\lambda_{ci} + \lambda_{ci-1})/2 \tag{22}$$

$$\Delta C_x = (\Delta C_i - \Delta C_{i-1})/\Delta x \tag{23}$$

$$k2\Delta D = k2_{i-1/2}(\Delta D_i + \Delta D_{i-1})/2 \tag{24}$$

$$\alpha\bar{u}^n \Delta a = \alpha_{i-1/2}(\bar{u}_i^n \Delta a_i + \bar{u}_{i-1}^n \Delta a_{i-1}^n)/2 \tag{25}$$

and so on; all of the terms in Eq. (17) are evaluated instead at the center of the mesh immediately preceding or following the x_i gridpoint, according to whether the local Mach number M_i is greater or lower than 1, respectively. For example, we have

$$\lambda_d = (\lambda_{di} + \lambda_{di-s})/2 \tag{26}$$

$$\Delta D_x = s(\Delta D_i - \Delta D_{i-s})/\Delta x \tag{27}$$

with $s = \text{sign}(M_i^n - 1)$. Notice that the incompressible flow coefficients and α, which are known analytically, are evaluated at the center of the mesh, whereas all of the other terms, which are computed numerically, are averaged from gridpoint values. Also, it has been found that approximating the terms of the type $\alpha\bar{u}^n\Delta a$ as in Eq. (25) produces a dramatic increase of the convergence rate of the numerical solution with respect to using the formally equivalent discretization

$$\alpha\bar{u}^n \Delta a = \alpha_{i-1/2}(\bar{u}_{i-1}^n + \bar{u}_i^n)(\Delta a_{i-1} + \Delta a_i)/4 \tag{28}$$

It needs to be remarked that the use of an upwind box-type discretization, as described above, causes a difficulty whenever a transition mesh is present, namely, a mesh in which the flow becomes supersonic or subsonic. In the first

case, the same spatial discretization of Eq. (17)—averaged at the center of the transition mesh—would be employed twice, since the two gridpoints immediately preceding and following such a mesh are characterized by subsonic and supersonic flow conditions, respectively; the resulting linear system to be solved would thus become indeterminate, leading to a failure of the numerical solution. In order to avoid such a breakdown of the method, Eq. (17) is discretized in space locally at the two aforementioned gridpoints, using a two-point first-order-accurate upwind difference for ΔD_x and a three-point second-order-accurate upwind difference for $\bar{D}_x^n$, so that the final steady-state solution remains second-order accurate in space. In the second case, i.e., when a shock is present in the transition mesh, the shock-tracking procedure by Moretti[6] is used to determine the position and velocity of the shock as well as to account for the discontinuities that the entropy and the C variable experience through the shock. However, since λ_c is also discontinuous through the shock and cannot therefore be averaged over the two neighboring gridpoints, Eq. (16) is discretized in space locally at the gridpoint immediately following the shock.

The boundary conditions are finally prescribed as follows. At the inlet of the nozzle, where only subsonic flow conditions are presently of interest, only one condition needs to be prescribed, namely, the value of the total speed of sound a_0. The boundary condition at the inlet gridpoint x_1 is, therefore,

$$\zeta a_1^2 + u_1^2 = \zeta a_0^2 \tag{29}$$

Equation (29) is written in terms of the perturbative variables and simplified by means of Eq. (9) to give

$$\zeta \bar{a}_1^2 + \bar{u}_1^2 + 2\zeta a_1' \bar{a}_1 + 2u' \bar{u}_1 = 0 \tag{30}$$

Eq. (30) is then written in incremental form and linearized to provide the sought boundary condition

$$2\zeta \bar{a}_1^n \Delta a_1 + 2\bar{u}_1^n \Delta u_1 + 2\zeta a_1' \Delta a_1 + 2u_1' \Delta u_1$$
$$= -\zeta (\bar{a}_1^n)^2 - (\bar{u}_1^n)^2 - 2\zeta a_1' \bar{a}_1^n - 2u_1' \bar{u}_1^n \tag{31}$$

Obviously, like in the case of the internal gridpoints, Δa_1 and Δu_1 are eliminated in favor of ΔC_1 and ΔD_1 by means of Eqs. (19) and (20). At the outlet of the nozzle, where again only subsonic flow conditions are of interest, the pressure is prescribed. By means of the isentropic condition and accounting for the entropy jump across the shock, if present, the outlet speed of sound a_{out} can be easily determined. Therefore, the boundary condition at the last gridpoint x_I is

$$\Delta a_I = a_{\text{out}} - a_I' - \bar{a}_I^n \tag{32}$$

The discrete internal and boundary equations, obtained as described above, provide a linear 2×2 block tridiagonal system for the $2I$ unknowns, $C_1, C_2, \ldots, C_I, D_1, D_2, \ldots, D_I$, which is solved very efficiently by standard block tridiagonal elimination.[12] The solution is then updated by means of Eqs. (18) and the process is repeated until a satisfactory convergence is reached.

Results

The present approach has been applied to compute several one-dimensional nozzle flows. A converging, a diverging, and a converging-diverging subsonic nozzle flows, as described in Ref. 6, have been considered at first, in order to compare the present method with the very accurate and efficient one proposed by Moretti.[6] A fourth, converging-diverging subsonic nozzle flow has also been considered, whose geometry is described later in the section devoted to the two-dimensional-flow results (see Fig. 5). The first two and the fourth nozzle flows have been computed using a uniform mesh with 9 gridpoints, whereas the third (converging-diverging) nozzle flow has been computed using a finer mesh with 23 gridpoints. The numerical results obtained by means of the present perturbative approach are given in Table 1, as the root mean square errors (with respect to the exact solution) for the pressure ϵ_P and the velocity ϵ_u, together with the corresponding ones (ϵ_P'', ϵ_u'') obtained by Magi and Vacca[13] using a nonperturbative version of this method and the same meshes.

From the results in Table 1, it appears that an error reduction of about 2-10 times is obtained for the different cases for both the pressure and the velocity when using the perturbative approach. As far as the efficiency (convergence rate) of the present computations is concerned, Table 2 provides the number of iterations (time steps) z necessary for the root mean square of Δu (Δurms) to become less that 1.E-7, together with the value of Δurms obtained after z iterations.

It is noteworthy that such a remarkable convergence rate is due to both the box-type spatial discretization and the implicit coupling of the governing equations used in the present numerical technique, as well as to the use of very large values of Δt. A comparable convergence rate has been obtained, in fact, by Magi and Vacca[13] applying the same numerical scheme to the original lambda equations.

A transonic nozzle flow case has been finally considered in order to test the present methodology when combined with the shock-tracking method of Moretti.[6] A nozzle having a dimensionless cross-sectional area $W = x/2 + 1/x$ ($0 \le x \le 3$), with a unitary inlet total pressure and an outlet static pressure equal to 0.75 has been used to this purpose. The same problem had been already solved in Ref. 3, where only the range ($0.6 \le x \le 3$) of the nozzle was computed in order to avoid the

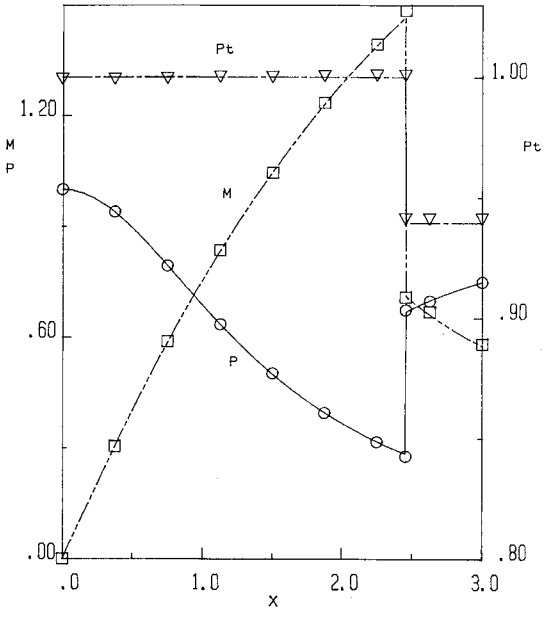

Fig. 1 Results for transonic nozzle flow.

Table 1 Subsonic nozzle flow results

Nozzle	ϵ_P	ϵ_u	ϵ_P''	ϵ_u''
1	3.76 E-5	1.20 E-4	1.12 E-4	2.82 E-4
2	1.04 E-4	1.76 E-4	1.15 E-3	1.82 E-3
3	1.16 E-3	1.97 E-3	2.21 E-3	3.28 E-3
4	7.53 E-4	1.49 E-3	3.54 E-3	7.47 E-3

Table 2 Subsonic nozzle flow convergence results

Nozzle	1	2	3	4
z	4	5	6	4
Δurms	8.4 E-10	8.5 E-9	9.0 E-9	7.8 E-12

breakdown of the method as the Mach number approaches zero near $x=0$. The results obtained using the present perturbative method and a very coarse (nine gridpoints) uniform mesh are given in Fig. 1, where the Mach number, pressure, and total pressure obtained numerically (symbols) are plotted vs the corresponding exact solutions (lines). The agreement is excellent, verifying the great accuracy of the proposed approach, even for transonic flows. Notice that the two symbols delimiting the shock are extrapolated from the neighboring gridpoint values (see Ref. 6 for details).

The convergence rate of the method is, of course, somewhat slowed down by the presence of the shock, which must be detected and tracked. However, a remarkable efficiency is still obtained, insofar as a satisfactory convergence has been obtained for the present transonic flow calculation in less than 20 iterations; see Fig. 2, where the location of the shock and its Mach number are plotted vs the number of iterations.

In all cases, the present method required less computational work (CPU time) than the already very efficient fast solver of Moretti[6] to achieve a comparable convergence level.

Two-Dimensional Flows

Numerical Method

For the case of two-dimensional flows, the lambda-formulation equations in a general orthogonal curvilinear coordinate system are given in Ref. 4. An appropriate "incompressible flow," $V'(v_1', v_2')$, a', is then considered, which is the solution of the following equations:

$$\mathrm{div}V' = \mathrm{curl}V' = 0 \tag{33a,b}$$

$$v_1'^2 + v_2'^2 + \zeta a'^2 = \zeta a_0^2 \tag{34}$$

It is noteworthy that the incompressible velocity V' and "speed of sound" a' are uncoupled and that a' can be evaluated [once the velocity field has been computed by solving Eqs. (33)] by means of the algebraic equation (34), in much the same manner as the pressure is obtained by means of Bernoulli equation in the case of classical incompressible flows. The incompressible flow, as defined above, is now used to define appropriate perturbative bicharacteristic variables as

$$\bar{C} = \bar{v}_1 + \zeta\bar{a} \tag{35}$$

$$\bar{D} = \bar{v}_1 - \zeta\bar{a} \tag{36}$$

$$\bar{E} = \bar{v}_2 + \zeta\bar{a} \tag{37}$$

$$\bar{F} = \bar{v}_2 - \zeta\bar{a} \tag{38}$$

where $\bar{v}_1$, $\bar{v}_2$, and $\bar{a}$ are obviously the differences between the compressible and incompressible velocity components and speed of sound, respectively. The two-dimensional perturbative lambda-formulation equations can finally be obtained, by means of some lengthy algebra, as

$$\bar{C}_t + \bar{D}_t + \frac{v_1+a}{h_1}\frac{\partial\bar{C}}{\partial q_1} + \frac{v_2}{h_2}\frac{\partial\bar{C}}{\partial q_2} + \frac{v_1-a}{h_1}\frac{\partial\bar{D}}{\partial q_1} + \frac{v_2}{h_2}\frac{\partial\bar{D}}{\partial q_2}$$
$$= \frac{2\bar{v}_2}{h_1 h_2}\left(\frac{\partial h_2}{\partial q_1}\bar{v}_2 + \frac{\partial h_1}{\partial q_2}\bar{v}_1\right) - k5_{1,2}\bar{v}_1 - k6_{1,2}\bar{v}_2 - k7_1\bar{a} \tag{39}$$

Table 3 $M=0.01$ elliptic channel flow results

Mesh	ϵ_{PT}	ϵ_P
8×4	6.2 E-9	5.8 E-9
16×8	1.6 E-9	1.2 E-9
32×16	4.1 E-10	6.2 E-10

$$\bar{E}_t + \bar{F}_t + \frac{v_1}{h_1}\frac{\partial\bar{E}}{\partial q_1} + \frac{v_2+a}{h_2}\frac{\partial\bar{E}}{\partial q_2} + \frac{v_1}{h_1}\frac{\partial\bar{F}}{\partial q_1} + \frac{v_2-a}{h_2}\frac{\partial\bar{F}}{\partial q_2}$$
$$= \frac{2\bar{v}_1}{h_1 h_2}\left(\frac{\partial h_1}{\partial q_2}\bar{v}_1 - \frac{\partial h_2}{\partial q_1}\bar{v}_2\right) - k5_{2,1}\bar{v}_1 - k6_{2,1}\bar{v}_2 - k7_2\bar{a} \tag{40}$$

$$\frac{1}{2}(\bar{C}_t - \bar{D}_t + \bar{E}_t - \bar{F}_t) + \frac{v_1+a}{h_1}\frac{\partial\bar{C}}{\partial q_1}$$
$$- \frac{v_1-a}{h_1}\frac{\partial\bar{D}}{\partial q_1} + \frac{v_2+a}{h_2}\frac{\partial\bar{E}}{\partial q_2} - \frac{v_2-a}{h_2}\frac{\partial\bar{F}}{\partial q_2}$$
$$= -\frac{2\bar{a}}{h_1 h_2}\left(\frac{\partial h_2}{\partial q_1}\bar{v}_1 + \frac{\partial h_1}{\partial q_2}\bar{v}_2\right) - k8_{1,2}\bar{v}_1 - k8_{2,1}\bar{v}_2 - k9 \tag{41}$$

$$\bar{C} - \bar{D} - \bar{E} + \bar{F} = 0 \tag{42}$$

In Eqs. (39-41), the subscript t indicates partial derivatives with respect to time, q_1, q_2, h_1, and h_2 are general orthogonal curvilinear coordinates and their corresponding scale factors,[14] and the k coefficients are functions only of the incompressible flow solution and of the coordinate system, so that they are constant with respect to time, and are given as

$$k5_{i,j} = \frac{2}{h_i}\left(\frac{\partial h_i}{\partial q_j}\frac{v_j'}{h_j} + \frac{\partial v_i'}{\partial q_i}\right) \tag{43}$$

$$k6_{i,j} = \frac{2}{h_j}\left(\frac{h_j}{h_i}\frac{\partial v_j'}{\partial q_i} - \frac{\partial h_j}{\partial q_i}\frac{v_j'}{h_i}\right) \tag{44}$$

$$k7_i = \frac{2\zeta}{h_i}\frac{\partial a'}{\partial q_i} \tag{45}$$

$$k8_{i,j} = \frac{2}{h_i}\left(\zeta\frac{\partial a'}{\partial q_i} + \frac{\partial h_j}{\partial q_i}\frac{a'}{h_j}\right) \tag{46}$$

$$k9 = 2\zeta\left(\frac{\partial a'}{\partial q_1}\frac{v_1'}{h_1} + \frac{\partial a'}{\partial q_2}\frac{v_2'}{h_2}\right) \tag{47}$$

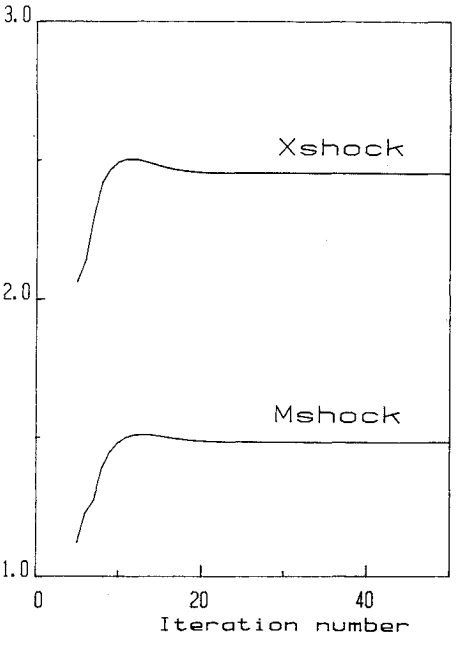

Fig. 2 Convergence history for transonic nozzle flow.

It is noteworthy that the present perturbative equations have a structure very similar to that of the standard lambda equations of Ref. 4; the only additional terms, as in the one-dimensional flow case, are those associated with the k coefficients and contain the unknown perturbative variables only as linear source (undifferentiated) terms. Furthermore, the coefficients of the advection terms are given in terms of the full compressible flow variables, v_1, v_2, and a, insofar as they provide the slopes of the physical bicharacteristic lines.

Equations (39-42) are discretized in time by means of a two-level Euler time stepping, using the delta form.[11] However, for the present case of two-dimensional flows, only the derivatives of the perturbative bicharacteristic variables in Eqs. (39-41) and all the terms in Eq. (42) are evaluated at the new time level (implicitly), whereas the other terms are all evaluated at the old time level (explicitly). For example, Eqs. (39) and (42) become

$$\frac{\Delta C}{\Delta t}+\frac{\Delta D}{\Delta t}+\frac{(v_1+a)^n}{h_1}\frac{\partial \Delta C}{\partial q_1}+\frac{v_2^n}{h_2}\frac{\partial \Delta C}{\partial q_2}$$

$$+\frac{(v_1-a)^n}{h_1}\frac{\partial \Delta D}{\partial q_1}+\frac{v_2^n}{h_2}\frac{\partial \Delta D}{\partial q_2}=\text{SSEQN(39)}^n \qquad (48)$$

where SSEQN(39)^n is a shorthand notation for steady-state Eq. (39) evaluated at the old time level t^n, and

$$\Delta C-\Delta D-\Delta E+\Delta F=0 \qquad (49)$$

respectively.

The resulting equations are then discretized in space using two-point first-order-accurate upwind differences for the incremental (Δ) derivatives and three-point second-order-accurate upwind differences for the derivatives in the right-hand sides of the equations, so that the final steady-state solution is second-order accurate. After eliminating the ΔF unknowns at all gridpoints by means of Eq. (49), a large block-pentadiagonal linear system is obtained. Such a system is factorized by a two sweep block-ADI method[4] so that a 3×3 block-tridiagonal system is solved along each row and column of the computational grid to evaluate ΔC, ΔD, and ΔE at all gridpoints. All of the perturbative variables and v_1, v_2, and a are finally updated and the process is repeated until a satisfactory convergence is obtained.

It is noteworthy that a fully implicit time discretization, like the one adopted for the case of one-dimensional flows, has been employed previously by the authors[3,4] for solving the lambda equations in two dimensions. Here it has been verified numerically that the present simpler approach converges in a slightly greater number of time steps, but requires less overall computer time, thanks to the reduced amount of computing to be performed at each single time step. Most likely, the convenience of this simpler method is due to the ADI factorization used to solve the large 3×3 block-pentadiagonal linear system approximately. A fully implicit time discretization, in fact, would probably improve the efficiency of the calculations, if an inexpensive direct solver were available, as in the one-dimensional case. Furthermore, it seems appropriate to point out that the incompressible flow velocity field V' being readily available when using the potential flow net as a suitable computational grid,[4] the additional computational cost required for solving the perturbative equations is negligible for the present case of an implicit integration scheme. In fact, the k coefficients are evaluated once and for all at the beginning of the computation and therefore only 8 extra multiplications and 12 extra additions need to be performed at every gridpoint and time step to evaluate the additional terms in the equations and to update the additional variables v_1, v_2, and a.

As far as the boundary conditions are concerned, the computational grid is always chosen to be the flow net of the incompressible potential flow V'. Therefore, the solid boundaries are always aligned with the coordinate lines (q_1) so that $\bar{v}_2=0$ at all of the solid-wall gridpoints. For the case of subsonic flows of interest here, two boundary conditions need to be prescribed at the inlet boundary, whereas only one is required at the outlet boundary. At the inlet, the total speed of sound is always imposed, together with the direction of the velocity vector V, which is assumed to be parallel to V'. Since the inlet boundary coincide with a potential line for the incompressible flow and is orthogonal to its streamlines, this second boundary condition becomes $\bar{v}_2=0$. Finally, at the outlet gridpoints, either the pressure (speed of sound) or its streamwise derivative is prescribed. At all boundary gridpoints, the appropriate boundary conditions (which are all physical ones) are used to eliminate from the governing equations those derivatives that involve gridpoints external to the flow domain. For example, at the outlet boundary, the derivatives of the D variable with respect to q_1 cannot be computed and are thus eliminated using the prescribed pressure condition. A more detailed discussion of boundary conditions is given in Ref. 4.

The initial condition for all of the calculations later presented in this paper is, of course, the incompressible flow solution V', a', so that all perturbative variables are zero at the initial time level.

Results

The compressible flow inside the channel comprised between two ellipses (having semiaxes equal to 1, 0.8, 1.85, and 1.75) has been considered at first in order to verify if the pres-

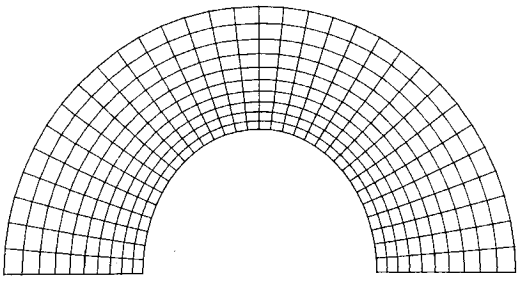

Fig. 3 Geometry and (32×10) computational mesh of the elliptic channel.

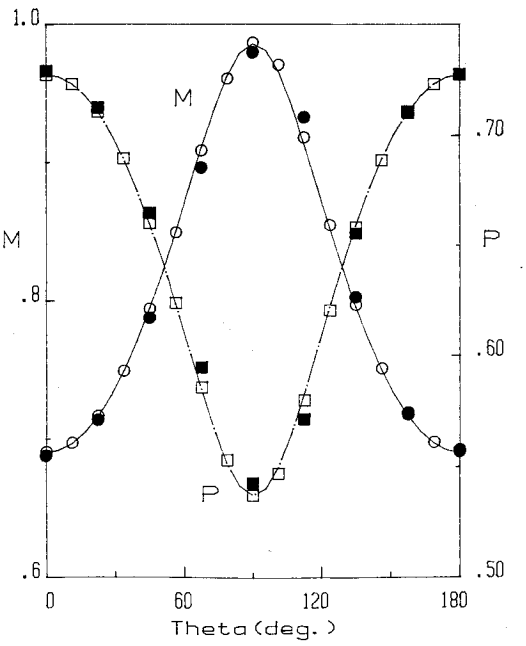

Fig. 4 Results for $M=0.69$ flow inside the elliptic channel.

ent perturbative approach could provide more accurate results than those, already remarkable, obtained in Ref. 4. The elliptic channel is first mapped into a circular one and then into a rectangle, by means of successive Joukowsky transformations (as was done in Ref. 4), so that a uniform Cartesian grid is obtained in the computational plane, corresponding to the incompressible potential flow net in the physical plane. The geometry of the channel as well as one of the computational meshes (32×10) employed in this study are given in Fig. 3.

Three flow cases have been considered, characterized by values of the inlet Mach number at the surface of the inner ellipse equal to 0.01, 0.2, and 0.69, so as to consider flowfields ranging from practically incompressible to almost critical conditions. For the lowest Mach number flow case, the results obtained using the present perturbative formulation and three different meshes are given as the root mean square errors for the total pressure ϵ_{PT} and the pressure ϵ_P with respect to the exact incompressible flow solution, averaged over the entire computational domain.

From the results in Table 3, it appears that the method is second-order accurate, insofar as the error for the total pressure vanishes as the square of the mesh size, and that the very coarse (8×4) mesh already provides extremely good accuracy; also, the errors for the pressure are extremely low, but do not vanish quadratically, the exact pressure being different from the incompressible one due to the nonzero compressibility effects. Obviously, no solution could be obtained at such a very low Mach number by means of the standard lambda method of Ref. 4.

For the $M=0.2$ and 0.69 flow cases, results have been obtained by means of both the present perturbative approach and the standard one,[4] using three different meshes. The results are given in Tables 4 and 5 as the root mean square errors along the surface of the inner ellipse for the total pressure ϵ_{PT}, the pressure ϵ_P, and the Mach number ϵ_M. It needs to be pointed out that, whereas the total pressure errors are computed with respect to the unitary exact solution, the other errors are computed with respect to the numerical solutions obtained using the same method and the finest (32×10) mesh. Also, a zero streamwise pressure derivative has been imposed at all of the outlet gridpoints, except one, where the pressure itself is prescribed, in all present calculations (see Ref. 4 for details). From the results in Tables 4 and 5, the following conclusions can be drawn:

1) The perturbative approach consistently provides more accurate solutions, especially for the coarser meshes and for the lower value of the Mach number.

2) The total pressure results obtained using the perturbative method show that the dominant gradients in the flowfield take place along the streamwise direction, insofar as ϵ_{PT} is seen to vanish just about as the square of the mesh size in that direction.

In order to provide a clearer evidence of the accuracy of the present methodology, the pressure and Mach number distributions along the wall of the inner ellipse are plotted vs the angle theta (corresponding to the circular channel obtained after the first Joukowsky transformation) in Fig. 4 for the most relevant $M=0.69$ flow case. The solutions obtained using both the very coarse (8×4) mesh (solid symbols) and the rather coarse (16×7) mesh (open symbols) are compared with the very accurate solutions (solid lines) obtained using the (32×10) mesh of Fig. 3. In spite of the considerable compressibility effects (the maximum Mach number is almost equal to one), the solution with the coarsest mesh is already acceptable and that with the intermediate mesh is very satisfactory. It is noteworthy that the three flow cases considered above have also been computed using a Dirichlet boundary condition for the pressure at the outlet of the channel and gave equivalent results.

A second channel flow, proposed by Moretti[15] as a severe subsonic flow problem, has then been considered. The channel is the symmetric one between a straight line and a circular arc and is depicted on Fig. 5, together with the finest computational mesh employed in this study. The straight wall of the channel goes from $x=-1.339$ to $x=1.339$, the circular arc has a radius equal to 1.919 and the minimum width of the channel (denoted here as "semicircular channel") is equal to 0.245. Only one flow case has been considered, namely, that corresponding to a unitary total pressure at the inlet of the channel and an outlet Mach number at the straight wall equal to 0.15. The results obtained using the proposed perturbative approach and three different meshes are given in Fig. 6 as the pressure and Mach number distributions along the circular

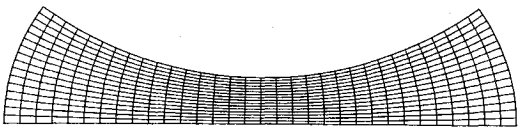

Fig. 5 Geometry and (32×16) computational mesh of the semicircular channel.

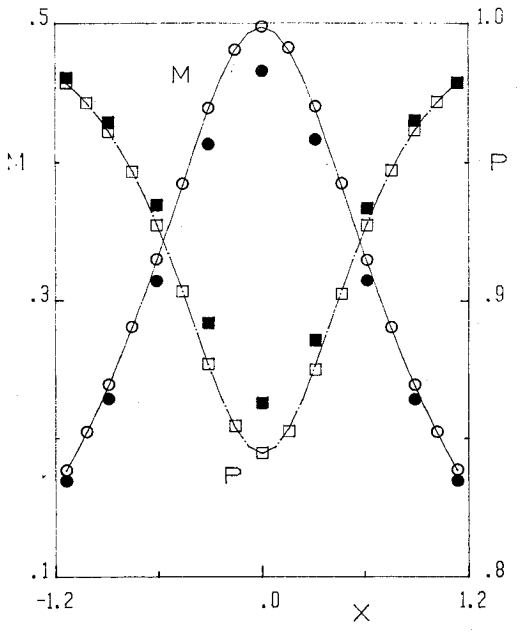

Fig. 6 Results for flow inside the semicircular channel.

Table 4 $M=0.2$ elliptic channel flow results

Mesh	Method	ϵ_{PT}	ϵ_P	ϵ_M
8×4	Perturb	1.25 E-4	6.44 E-5	1.49 E-6
	Standard	4.34 E-3	1.93 E-2	2.38 E-3
16×7	Perturb	1.99 E-5	1.33 E-5	2.57 E-8
	Standard	3.52 E-4	1.38 E-4	1.03 E-5
32×10	Perturb	4.93 E-6	—	—
	Standard	5.17 E-5	—	—

Table 5 $M=0.69$ elliptic channel flow results

Mesh	Method	ϵ_{PT}	ϵ_P	ϵ_M
8×4	Perturb	1.59 E-3	5.80 E-3	7.33 E-4
	Standard	6.97 E-3	6.02 E-3	1.18 E-3
16×7	Perturb	4.93 E-4	1.17 E-3	6.80 E-5
	Standard	5.80 E-4	1.18 E-3	6.06 E-5
32×10	Perturb	1.16 E-4	—	—
	Standard	2.15 E-4	—	—

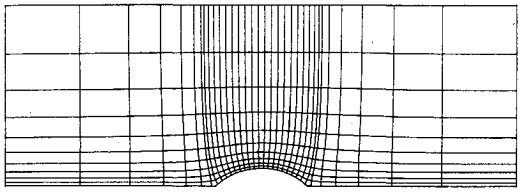

Fig. 7 Geometry and (33 × 10) computational mesh for the channel with a circular arc hump.

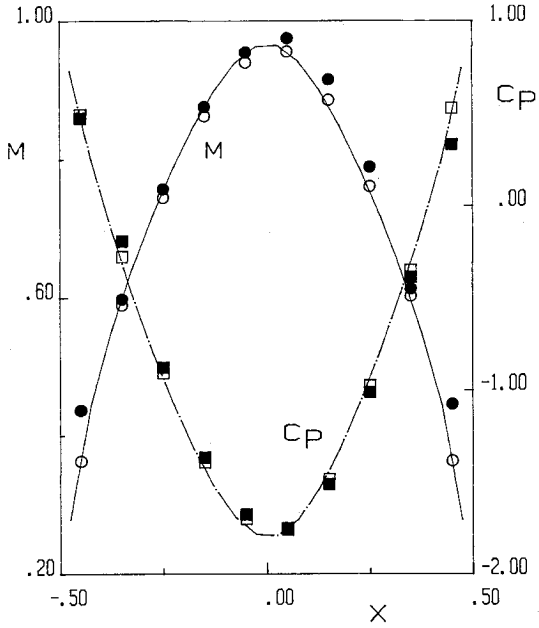

Fig. 8 Results for $M = 0.52$ flow inside the channel with a circular arc hump.

wall. The solid and open symbols indicate the results obtained using a very coarse (8 × 4) mesh and a rather coarse (16 × 8) mesh, respectively, whereas the solid lines indicate the fine (32 × 16) mesh results. The remarkable accuracy achieved also for such a difficult flow case once more demonstrates the validity of the proposed methodology. It is noteworthy that the present results have been obtained using a Dirichlet outlet boundary condition for the pressure (namely, $\bar{a} = 0$), insofar as the method experienced convergence problems when using a prescribed streamwise derivative for the pressure at the outlet of the channel.

Finally, the flow inside a plane channel with a circular hump was considered, in order to test the present method for a more general geometry, for which an analytical solution of the corresponding incompressible flow is not readily available. The geometry of the channel is given in Fig. 7, together with the potential flow net computational grid obtained by means of the numerical integration of the Schwartz-Christoffel transformation due to Davis.[16] The geometry is such that the height to chord ratio of the circular arc is equal to 0.2 and the ratio between the chord of the arc and the width of the channel is equal to 0.5. It is noteworthy that the computational grids used in this study are stretched ahead of and behind the hump, as well as in the transversal direction, but are uniform along the surface of the hump itself; see Fig. 7, which provides the finer (33 × 10) mesh employed for the present computations.

The quasicritical flow case corresponding to an upstream Mach number of 0.52 has been considered as a severe test for the proposed method. The results obtained using both the present perturbative approach and the standard lambda method of Ref. 4 are given in Fig. 8 as the Mach number and pressure coefficient distributions along the surface of the hump. The solid lines indicate the perturbative solution using the (33 × 10) mesh depicted in Fig. 8, whereas the solid and open symbols indicate the solutions obtained by means of the method of Ref. 4 and the present one, respectively, using a coarser (17 × 6) mesh. It clearly appears that the new method once more provides a considerable improvement in accuracy over the previous one. Incidentally, the average total pressure errors along the surface of the hump are about 2 and 0.4% for the nonperturbative and perturbative solutions, respectively, and only 0.1% for the perturbative solution using the finer (33 × 10) mesh.

As far as the efficiency of the present ADI method is concerned, a satisfactory convergence has always been obtained in about 50 iterations (time cycles), or less, the convergence rate and optimal CFL numbers being comparable to those of the similar standard technique of Ref. 4.

Conclusions

A perturbative lambda formulation has been provided for computing compressible one- and two-dimensional arbitrary internal flows. New sets of lambda equations have been derived in terms of perturbative characteristic-type variables, which are the differences between the standard Riemann variables and those corresponding to an appropriate incompressible flow. The governing equations have been solved numerically by means of a fully implicit method incorporating a shock-tracking procedure for one-dimensional flows and of a block ADI method for two-dimensional flows. The proposed approach has been shown to provide a significant accuracy improvement over the already very accurate lambda formulation. Current effort is devoted to modify the two-dimensional-flow method so as to extend its validity into the transonic flow range.[17]

Acknowledgments

This research has been supported by Ministero della Pubblica Istruzione and Consiglio Nazionale delle Ricerche. The original idea of a perturbative lambda formulation was born during a very stimulating discussion among Prof. R. T. Davis and the authors at the University of Cincinnati in July 1982.

References

[1]Moretti, G., "The λ-scheme," *Computers and Fluids*, Vol. 7, 1979, pp. 191-205.

[2]Zannetti, L. and Colasurdo, G., "Unsteady Compressible Flow: a Computational Method Consistent with the Physical Phenomena," *AIAA Journal*, Vol. 19, July 1981, pp. 851-856.

[3]Dadone, A. and Napolitano, M., "An Implicit Lambda Scheme," *AIAA Journal*, Vol. 21, Oct. 1983, pp. 1391-1399.

[4]Dadone, A. and Napolitano, M., "Efficient Transonic Flow Solutions to the Euler Equations," AIAA Paper 83-0258, 1983 (also, "An Efficient ADI Lambda Formulation," *Computers and Fluids*, to be published).

[5]Napolitano, M. and Dadone, A., "Implicit Lambda Methods for Three-Dimensional Compressible Flows," *AIAA Journal*, Vol. 23, Sept. 1985, pp. 1343-1347.

[6]Moretti, G., "Fast Euler Solver for Steady, One-dimensional Flows," NASA CR 3689, 1983 (also, *Computers and Fluids*, Vol. 13, 1985, pp. 61-81).

[7]Moretti, G., "A Fast Euler Solver for Steady Flows," AIAA Paper 83-1940, 1983.

[8]Dadone, A. and Napolitano, M., "Recenti Sviluppi sul Calcolo di Flussi Comprimibili non Viscosi," Paper presented at 38th ATI Congress, Bari, Italy, Sept. 1983.

[9]Chow, L. J., Pulliam, T. H., and Steger, J. L., "A General Perturbation Approach for the Equations of Fluid Dynamics," AIAA Paper 83-1903, 1983.

[10]Dadone, A. and Napolitano, M., "A Perturbative Lambda Formulation," *Ninth International Conference on Numerical Methods in Fluid Dynamics, Lecture Notes in Physics*, Vol. 218, Springer-Verlag, Berlin, New York, 1985, pp. 175-179.

[11]Beam, R. M. and Warming, R. F., "An Implicit Factored Scheme for the Compressible Navier-Stokes Equations," *AIAA Journal*, Vol. 16, April 1978, pp. 393-402.

[12]Isaacson, E. and Keller, H. B., *Analysis of Numerical Methods*, John Wiley & Sons, New York, 1966.

[13]Magi, V. and Vacca, G., "Calcolo di Flussi Unidimensionali non Isentropici Mediante Implicit Box Lambda-Scheme," Paper presented at 38th ATI Congress, Bari, Italy, Sept. 1983.

[14]Karamcheti, K., *Principles of Ideal Fluid Aerodynamics*, John Wiley & Sons, New York, 1966.

[15]Moretti, G., Private communication.

[16]Davis, R. T., "Notes on Numerical Methods for Coordinate Generation Based on a Mapping Technique," *VKI Lecture Series*, No. 5, 1981.

[17]Dadone, A. "Accurate and Efficient Solutions of Transonic Internal Flows," AIAA Paper 85-1334, 1985.